D22

N78-32488

A NASTRAN ANALYSIS OF A TOKAMAK VACUUM VESSEL USING INTERACTIVE GRAPHICS

by
Arthur Miller
Grumman Aerospace Corp.
and
Morris Badrian
EBASCO Services, Inc.

SUMMARY

A TAKOMAK Vacuum Vessel was analyzed using MSC/NASTRAN. Isoparametric quadrilateral and triangular elements were used to represent the Vacuum Vessel shell structure. For toroidally symmetric loadings, MPCs were employed across model boundaries and Rigid Format 24 was invoked. Un-symmetric loadings required the use of the cyclic symmetry analysis available with Rigid Format 49. NASTRAN served as an important analysis tool in the TOKAMAK design effort by providing a reliable means for assessing structural integrity. Interactive graphics were employed in the finite element model generation and in the post-processing of results. The authors feel that model generation and checkout with interactive graphics reduced the modelling effort and debugging man-hours significantly.

INTRODUCTION

This paper presents the structural modelling method, analysis procedures and results of a TOKAMAK Vacuum Vessel finite element analysis. The analysis described herein was required for the design-verification of the TOKAMAK FUSION TEST REACTOR (TFTR) Vacuum Vessel. The TOKAMAK is a toroidal device through which magnetic fields permeate to confine a plasma. The magnetic fields are produced by strong electric currents on the order of 40,000 amperes passing through both copper coils and the plasma. In the TOKAMAK, there are two major magnetic fields: a toroidal field generated by current flowing in the coils enveloping the torus, and a poloidal field generated by current flowing through both the plasma and an equilibrium field coil. By combining toroidal and poloidal magnetic fields, the TOKAMAK achieves a higher level of plasma stability than has been realized in any previous magnetic-confinement

system. The increased plasma stability permits longer confinement times of higher temperature plasmas. The TFTR will therefore come closer to meeting all necessary conditions for a net production of fusion energy than any previous magnetic fusion device. A basic function of the Vacuum Vessel is to provide containment of the hot (100 million degrees Celsius) Deuterium-Tritium plasma while excluding the atmosphere.

SYMBOLS

Values are given in both SI and US Customary Units. Calculations were made in US Customary Units.

f_b	Bending stress, psi (MPa)
f_{max}	Maximum combined stress, psi (MPa)
f_m	Membrane stress, psi (MPa)
f_{xy}	In-plane shear stress, psi (MPa)
F_x	Circumferential (toroidal) membrane load, lb/in. (N/m)
F_y	Meridional membrane load, lb/in. (N/m)
F_{xy}	In-plane membrane shear load, lb/in. (N/m)
Q_x	Transverse shear load (causing M_x bending), lb/in. (N/m)
M_x	Circumferential (toroidal) bending load, in lb/in. (N-m/m)
M_y	Meridional bending load, in. lb/in. (N-m/m)
q_x	Transverse shear stress, psi (MPa)
t	Material Thickness, in. (m)

THE TOKAMAK VACUUM VESSEL

The Vacuum Vessel (Fig. 1) is essentially a large doughnut-shaped vessel (or torus) composed of ten stainless steel segments joined at ten parting planes. Each segment contains five intersecting cylinders (three pie sections and two bellows cases) as shown in the plan view (Fig. 2). The diametral centerline of each cylindrical section intersects the vertical axis of symmetry of the machine. Six of the segments include a Neutral Beam Injection Duct, as shown in Figure 1. (The purpose of the Neutral Beam Injection Duct is to produce high-energy Deuterium atoms and to inject them into a magnetically-confined Tritium

plasma causing Deuterium-Tritium fusion reactions to occur.) Each segment is supported at both a radially inboard and a radially outboard location. Inboard supports supply essentially vertical restraint, supporting approximately 1/3 of the deadweight of the Vacuum Vessel. Outboard supports allow free radially inward displacement while restraining radially outward, toroidal and vertical motion.

FINITE ELEMENT IDEALIZATION

Two models of Vacuum Vessel segments have been developed which span from parting plane to parting plane. A derivative of the non-Neutral Beam Injection Duct model was also created for analysis of anti-symmetric loading. The first model, shown in Figure 3, contains detailed features such as diagnostic and access port extensions, non-structural port covers, the parting plane (P/P) weld thickness with its stiffening rings, the plasma limiter support structure, pie bellows-case (P/B) stiffening rings, and the inboard and outboard supports. QUAD4 and TRIA3 isoparametric plate bending elements were used for the shell idealization. (These elements were chosen because they provide superior results with fewer elements. The results of element test problems carried out by MSC (Ref. 1) has shown that the accuracy of the QUAD4 element is effectively independent of the aspect ratio.) Beam elements were used to simulate the stiffening rings at the P/B intersections, and those adjacent to the parting plane. These element types were also used to idealize the Vacuum Vessel supports and flanges at the ends of the port extensions. Rod elements were used to model the protrusions at the port-shell intersections. Continuity of the finite element model across structural interfaces (viz. at the P/B intersections, parting plane/ring intersections and at the vessel support connections) was achieved by means of rigid-bar and rigid-triangular elements. The second model as shown in Figures 4 and 5, is essentially the same as the first except for the inclusion of a Neutral Beam Injection Duct. Each model consisted of approximately 1900 nodes with 6 DOF at each node.

MODEL GENERATION WITH INTERACTIVE GRAPHICS

The interactive display feature of Control Data's UNISTRUC program facilitated the modelling of the numerous penetrations, eccentricities and extensions which comprise more than 60% of the total model. In order to develop this geometrically complex finite element idealization it was necessary to employ several pre-processors. (The sequence of steps employed in the model generation which are described below are schematically depicted in Figure 6.) First, a FORTRAN program was written to geometrically outline the boundaries of major individual structural components. The results of this program were input into UNISTRUC in terms of "lines" and "points". The boundary interiors were then meshed by employing UNISTRUC's generic element library (Ref. 2).

In addition to nodes and elements, loads, material properties and physical properties were defined and graphically reviewed through UNISTRUC. This information was written to a "Neutral Input File" in an application-independent format. Inputting this file to the "NASTRAN Input-File Translator" resulted in a file containing properly formatted Executive Control, Case Control and Bulk Data card images. To take advantage of more recent NASTRAN features which are not currently compatible with UNISTRUC (e.g. rigid elements) it was necessary to edit the card images. This was accomplished through the use of the INTERCOM interactive editing feature of Control Data's Scope 3.4 Operating System (Ref. 3). Model bandwidth optimization and SEQGP card generation was accomplished by a stand-alone optimizer residing on a linked mainframe, and subsequently merged, through INTERCOM, with the NASTRAN Bulk Data.

LOADINGS

The TFTR is subjected to several different loading combinations. These combinations include the Normal Operating Condition, Bakeout, Discharge Cleaning, Plasma Disruption, Seismic and Coil Short-circuiting. As of this writing the Vacuum Vessel has been analyzed for the severe conditions associated with a Plasma Disruption. A Plasma Disruption loading consists of electromagnetic centering forces, electromagnetic pressure and electromagnetically-induced toroidal and racking forces on the bellows case rings in addition to the

deadweight of the Vessel, and external pressurization. For the sake of brevity, this paper will only present results related to the gravity and pressurization subcase.

ANALYSIS PROCEDURE

Due to budgetary constraints it was decided early in the program not to model the entire torus structure. Instead, individual models consisted of a single segment type with boundary conditions selected so as to simulate a complete torus. Analysis with smaller models had shown that results of sufficient accuracy would be obtained with this idealization. For torcidally symmetric loadings, the most efficient analysis technique was to employ MPCs across the boundaries of the selected segment type and invoke Rigid Format 24. Unsymmetric loadings required the use of the more expensive Cyclic Symmetry Analysis available in Rigid Format 49. (A Cyclic Symmetric run with a harmonic index of five was found to require twice the CPU time and 3.5 times the I/O as compared to the MPC'd boundary model.) Based on the economic and technical resources available, it was decided to perform the analyses on a second mainframe containing the MSC/NASTRAN Version 40 operating under the Network Operating System/Batch Environment.

ANALYSIS RESULTS

The resulting significant internal membrane and bending force distributions are depicted in Figures 7 through 10. Continuity of the curves was obtained by smoothing the computer-output values at element centroids. In regions of load and/or structural discontinuity, the results were extrapolated to the edges of the finite elements under consideration. These results were checked, where feasible, by utilizing equilibrium and compatibility relationships, thus maximizing the information yielded by the analysis. Post processing of the results would have been more expeditious had an option been available in NASTRAN to print out element internal load intensities (Mx, My, Nx, Ny, Nxy, Qx, Qy) at the element corners in addition to the element centroid. This feature would more clearly define internal load gradients. Had this option been available, much of the time expended in manually smoothing and extrapolating the

results would have been saved. Figures 7 and 8 present the critical internal loads below the torus' horizontal axis of symmetry, specifically at the following critical locations: the maximum pie/bellows interface eccentricities and at the connection of the outboard supports to the torus. Figures 9 and 10 each present the internal loads along a meridian. Figure 9 depicts the axial and bending loads along the centerline of pie 2, while Figure 10 depicts the loads in the parting plane weld.

The relationship between the internal loads and the resulting stresses is as follows:

$$f_{max} = f_m \pm f_b = \frac{F_x}{t} \pm \frac{6M_x}{t^2}$$

$$\text{or } \frac{F_y}{t} \pm \frac{6M_y}{t^2}$$

} combined membrane and bending stresses

$$f_{xy} = \frac{F_{xy}}{t}$$ In-plane shear stress

$$q_x = \frac{Q_x}{t}$$ Transverse shear stress

where t = .5 inches (.0127 meters) applicable to Figures 7 thru 9
t = .312 inches (.00792 meters) applicable to Figure 10, parting plane weld

An inspection of the results indicates that the critical stresses occur in the following Vacuum Vessel locations:

-In Pies 1 and 2, at the maximum pie/bellows interface eccentricities, Figure 7.

$$fx_{max} = \frac{F_x}{t} + \frac{6M_x}{t^2} = \frac{-900}{.5} - \frac{6 \times 450}{(.5)^2} = \begin{matrix}-12,600 \text{ psi} \\ (-86.874 \text{ MPa})\end{matrix}$$

-In Pie 2, at the diagnostic port-shell intersection, Section A-A, Figure 8.

$$fx_{max} = \frac{Fx}{t} + \frac{6M_x}{t^2} = \frac{-4500}{.5} - \frac{6 \times 100}{(.5)^2} = \begin{matrix}-11,400 \text{ psi} \\ (-78.6 \text{ MPa})\end{matrix}$$

- In Pie 2, at the diagnostic port-shell intersection, Figure 9.

$$fy_{max} = \frac{Fy}{t} + \frac{6M_y}{t^2} = \frac{-2500}{.5} - \frac{6 \times 130}{(.5)^2} = \begin{matrix} -8120 \text{ psi} \\ (-55.9 \text{ MPa}) \end{matrix}$$

In the parting plane weld region, Figure 10, the Mx bending results are increased by 20% to account for moment peaking at the intersection of the 5/16 inch (.00794 meters) weld with the P/P stiffening ring:

$$fx_{max} = \frac{Fx}{t} + 1.2\,\frac{6M_x}{t^2} = \frac{-750}{.312} - 1.2\,\frac{6 \times 100}{(.312)^2} = \begin{matrix} -9800 \text{ psi} \\ (-67.57 \text{ MPa}) \end{matrix}$$

DEFLECTIONS

Grid point displacements, element forces and stress were output to the NASTRAN UT1 file by appropriate DMAP instructions generated by UNISTRUC. The contents of the UT1 file were transformed by means of the UNISTRUC file translator for compatibility with the UNISTRUC system, thus making interactive display of the results possible. Displays of the deflected shapes of major structural components appear in Figures 11 thru 16. A maximum deflection of .037 inches (0.00094 meters) occured at the intersection of the outside edge of the diagnostic port and the shell on Pie 2 as shown in Figure 14.

CONCLUSIONS

NASTRAN proved to be a valuable analysis tool for the design-verification of a TFTR Vacuum Vessel. Furthermore, it was found that analysis of a 1/10 segment of a structure with Rotational Cyclic Symmetry (K = 5) and non-symmetrical loading was approximately 2 1/2 times more costly than for a symmetrically loaded model of the same fundamental region with MPCs across the boundaries.

The use of interactive graphics in both the pre and post-processing modes was found to be an indispensible tool when dealing with complex three-dimensional models.

REFERENCES

1. MacNeal-Schwendler Corporation, MSC/NASTRAN Application Manual For CDC 6000 Series, Los Angeles, California.

2. Control Data Corporation, Unified Structural Design System (UNISTRUC), Version 1.2, Publication No. 76079600, Publications and Graphics Division, St. Paul, Minnesota.

3. Control Data Corporation, CYBERNET Service INTERCOM 4 Reference Manual, Publication No. 84000024, Publications and Graphics Division, Data Services Publications, Minneapolis, Minnesota.

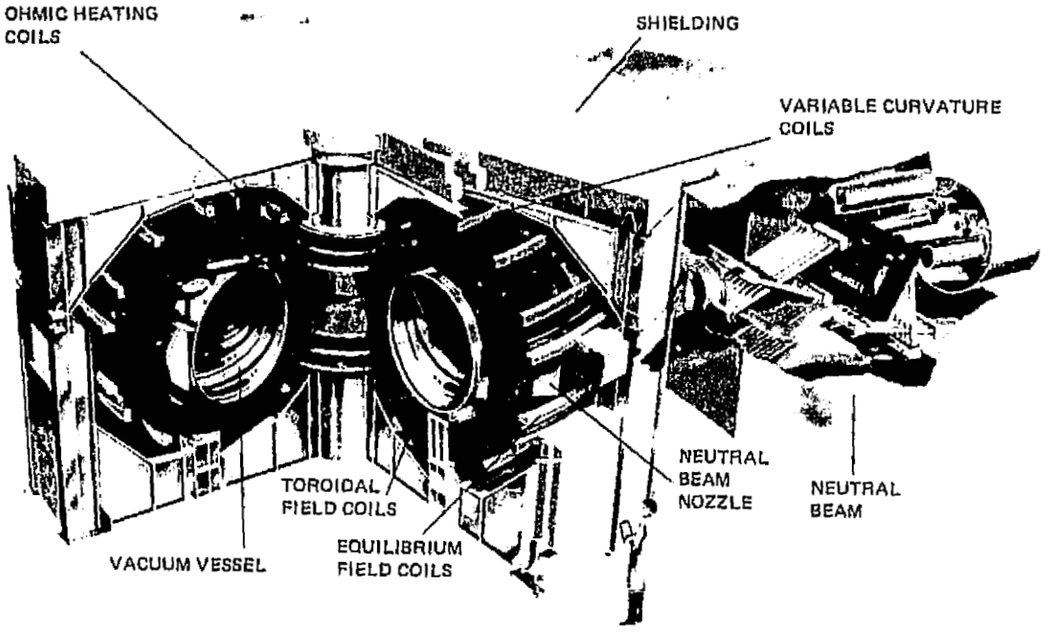

(a) Tokamak Fusion Test Reactor

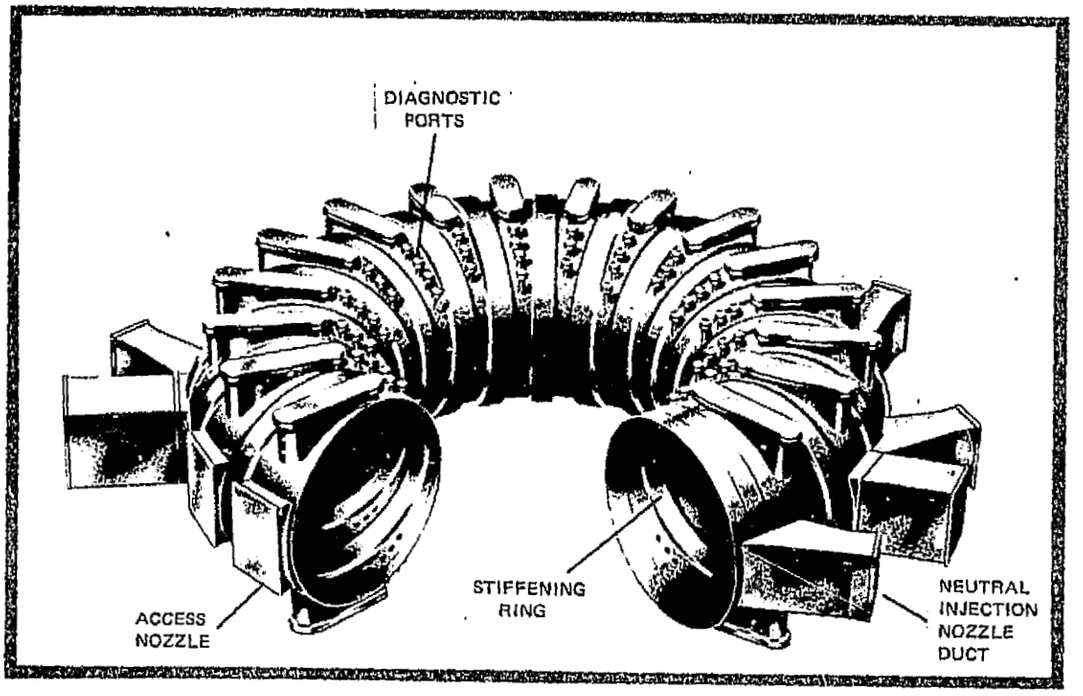

(b) Vacuum Vessel

2036-001

Figure 1 Tokamak Fusion Test Reactor – Vacuum Vessel

C-5

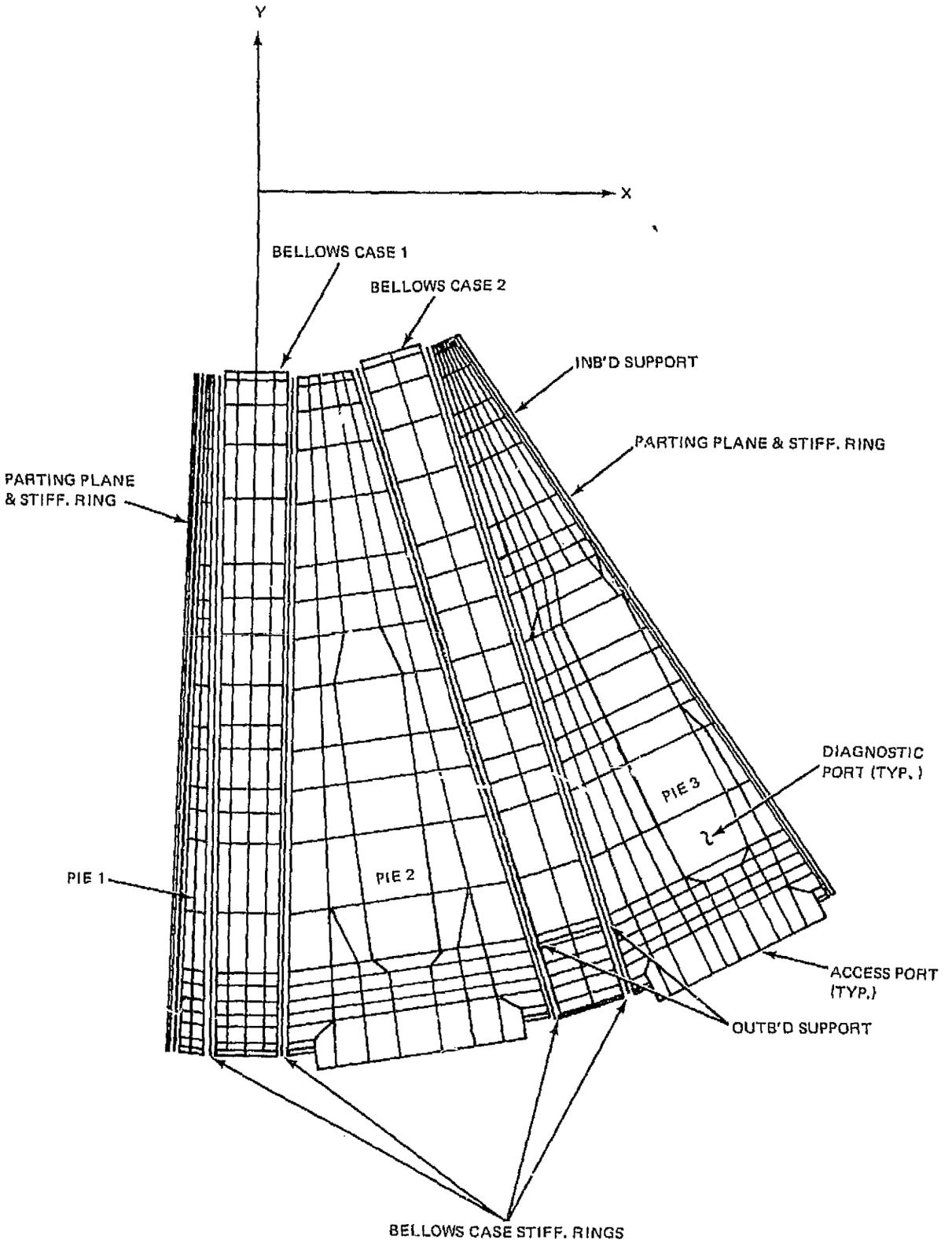

Figure 2 TFTR Vacuum Vessel – Finite Element Model, Plan View

ORIGINAL PAGE IS
OF POOR QUALITY

2036-003

Figure 3 TFTR Vacuum Vessel - Finite Element Model, Isometric View

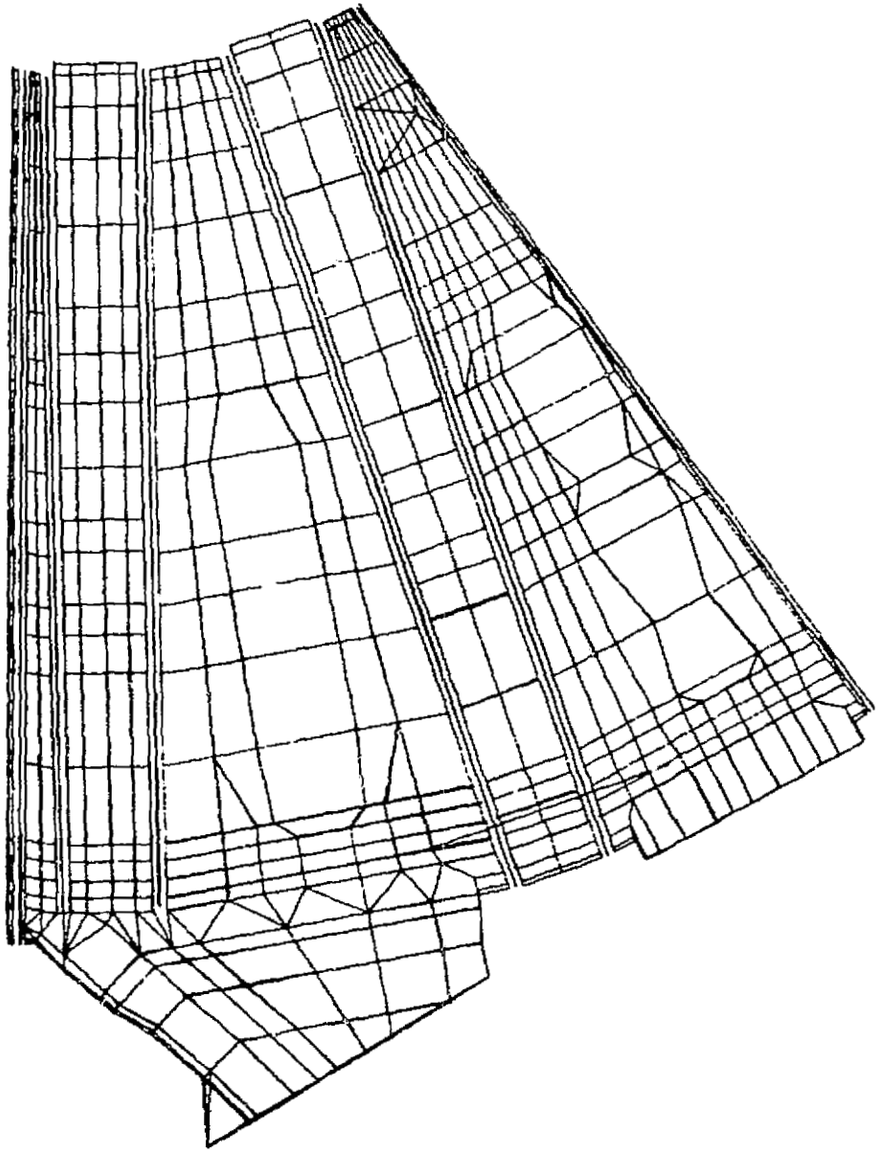

2036-004

Figure 4 Neutral Beam Duct Segment - Finite Element Model, Plan View

Figure 5 Neutral Beam Duct Segment - Finite Element Model, Isometric View

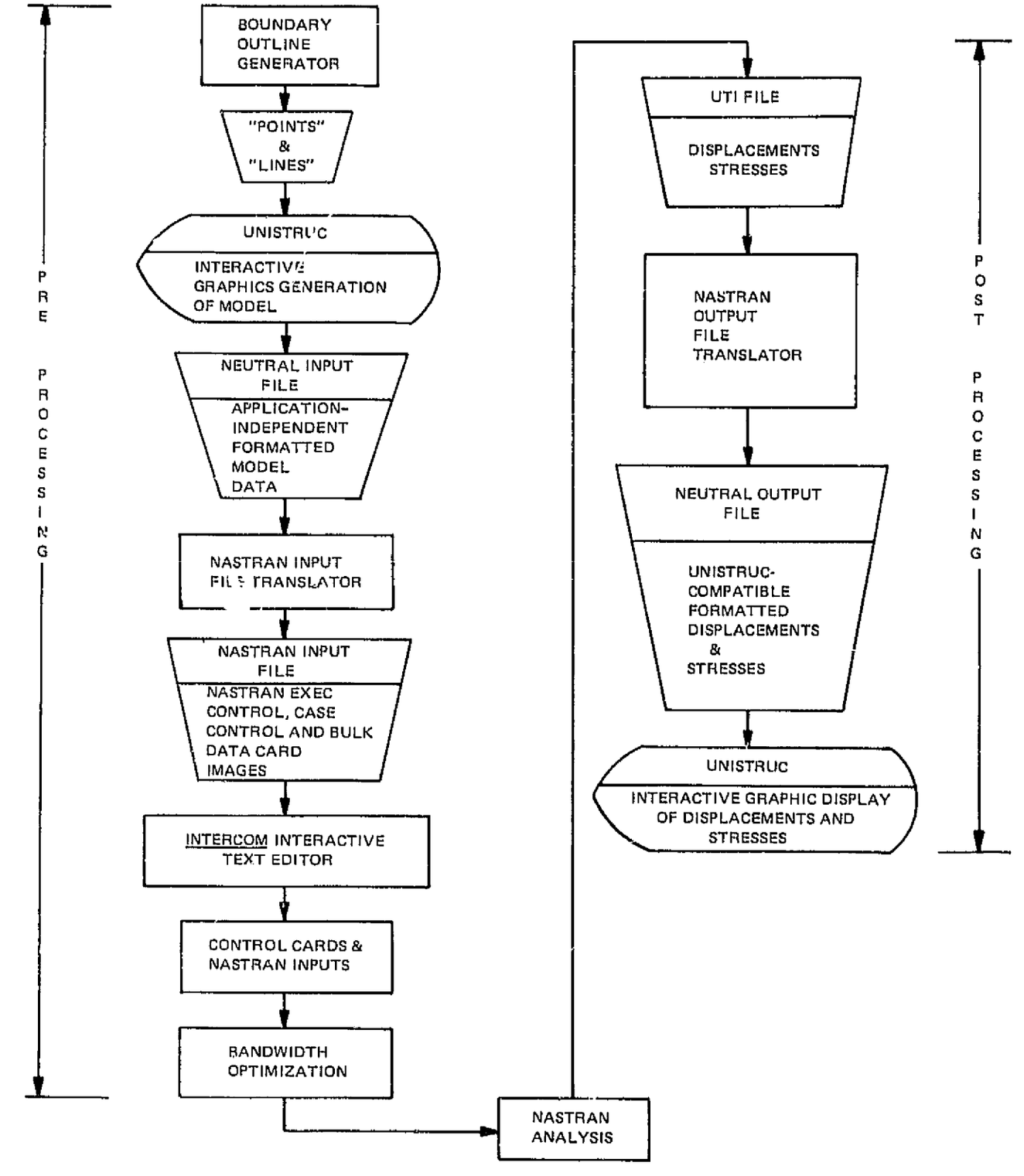

Figure 6 Pre and Post Processing with Interactive Graphics

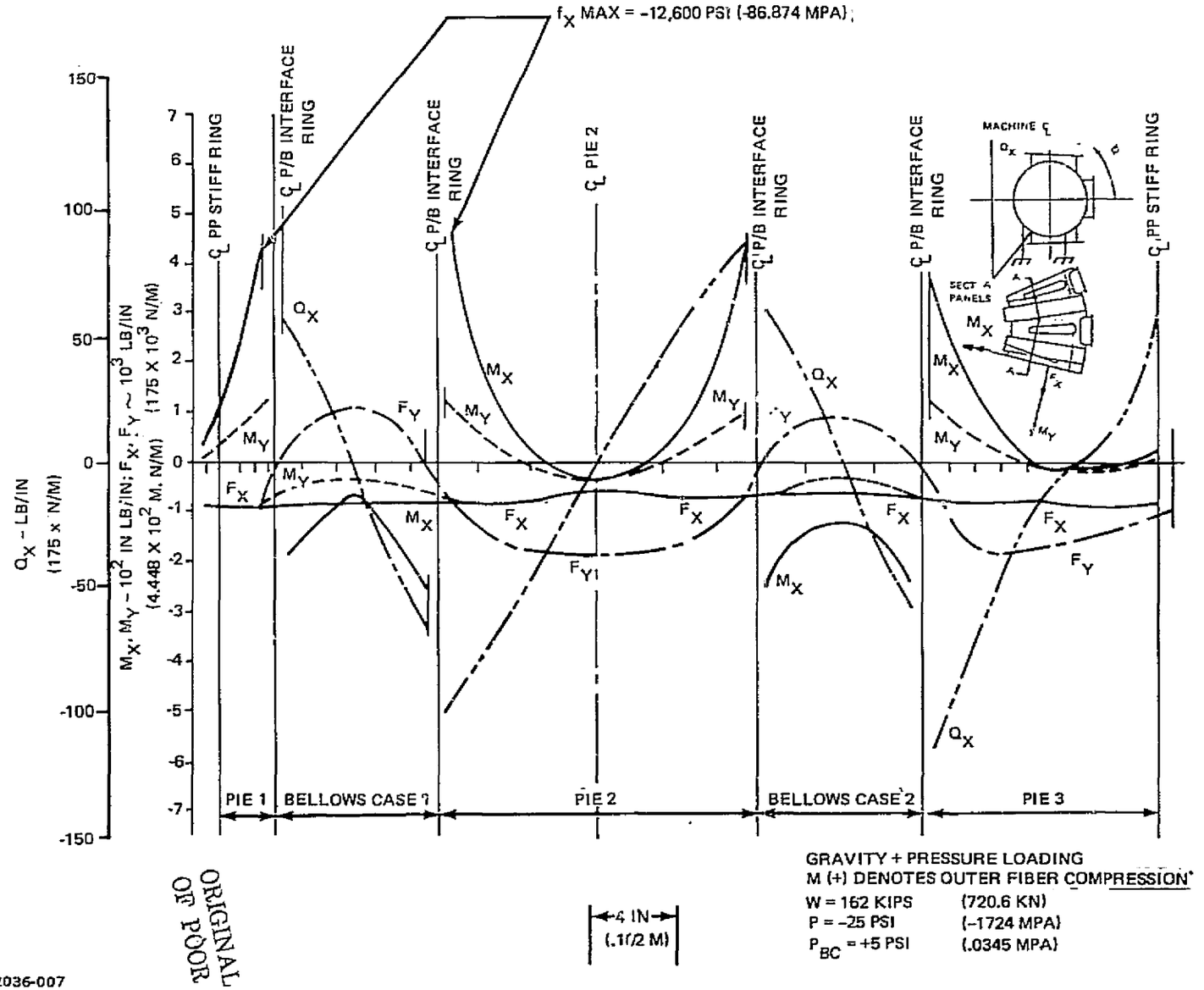

Figure 7 Loads at Maximum Pie/Bellows Case Interface Eccentricity

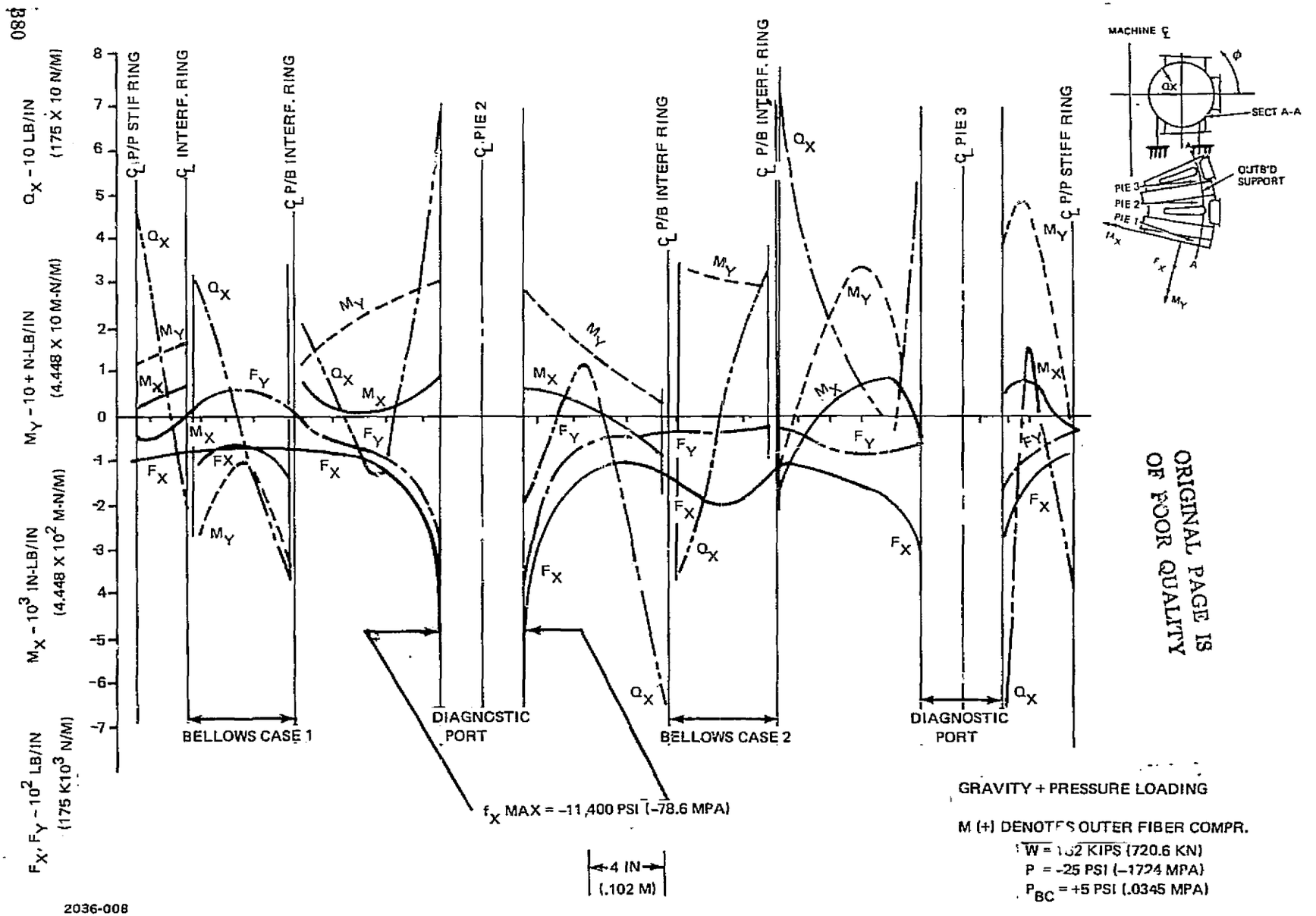

Figure 8 Loads at the Connection of the Outboard Supports to the Torus

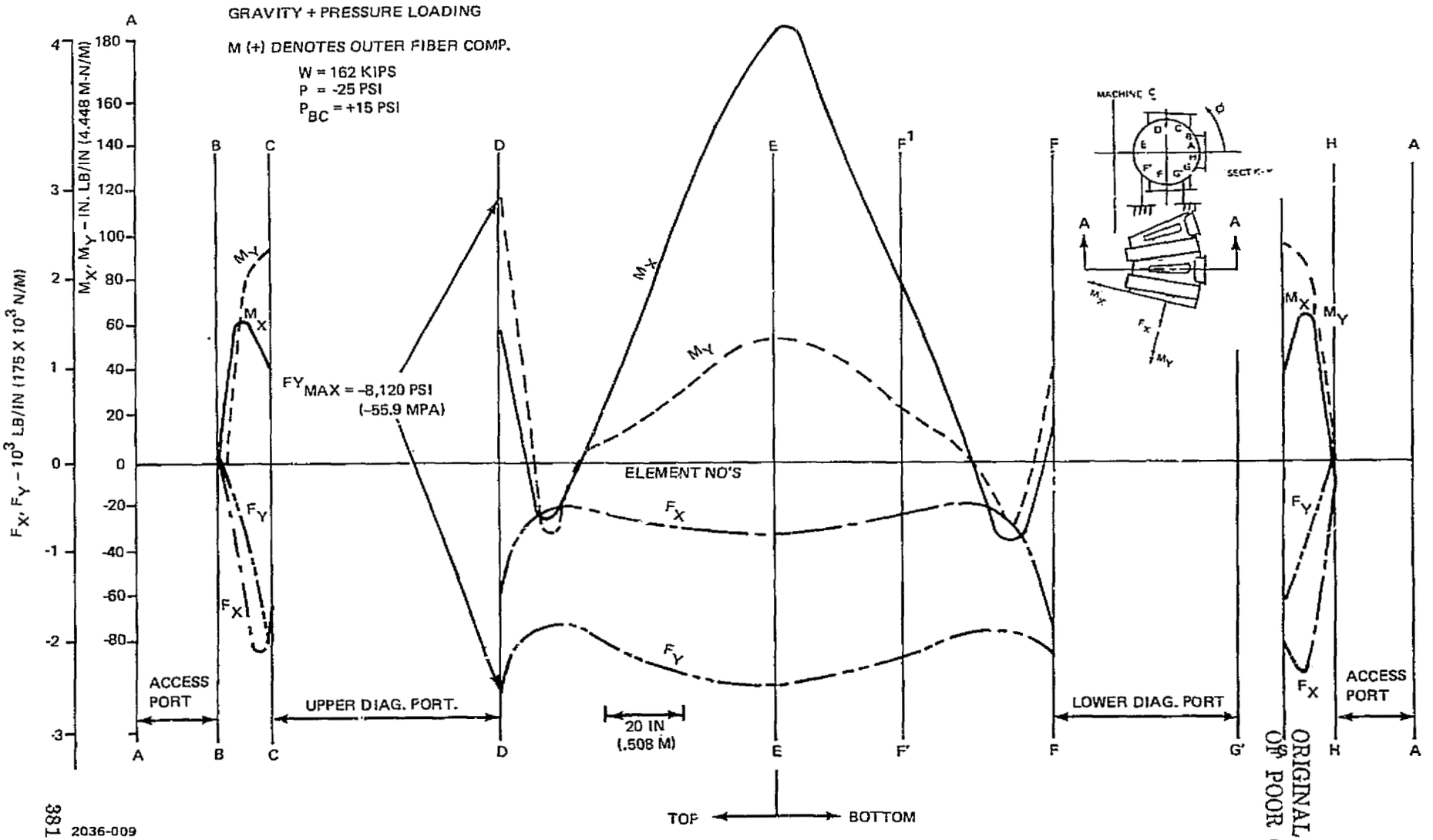

Figure 9 Loads Along the Centerline of Pie 2

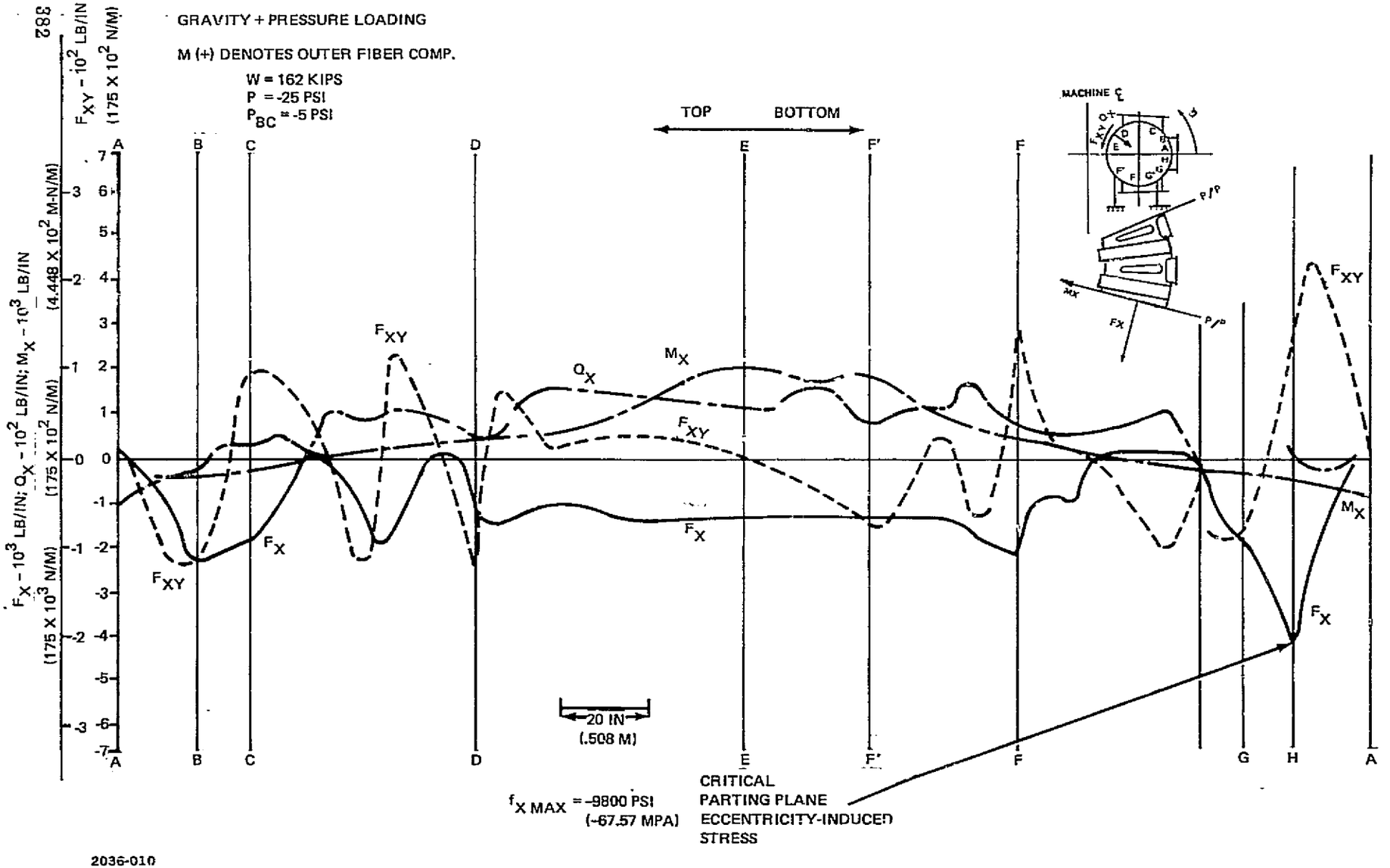

Figure 10 Loads in the Parting Plane Weld

LOAD CONDITION:
PRESSURE & GRAVITY

P_{SHELL} = -25 PSI (-.1724 MPa)

$P_{BELLOWS\ CASE}$ = + 5 PSI (.0345 MPa)

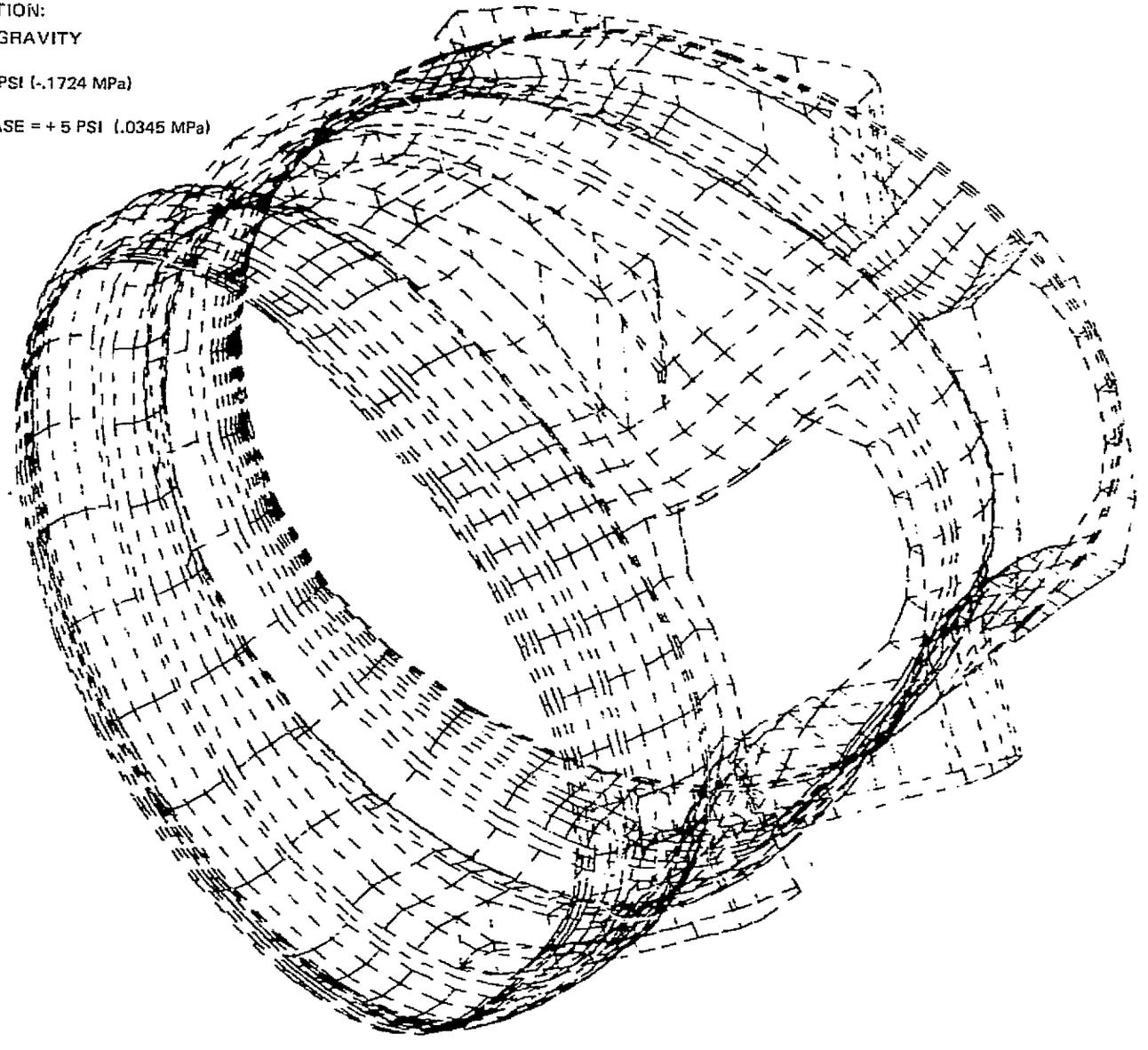

2036-011

Figure 11 Deformed Shape of TFTR Vacuum Vessel Finite Element Model, Isometric View

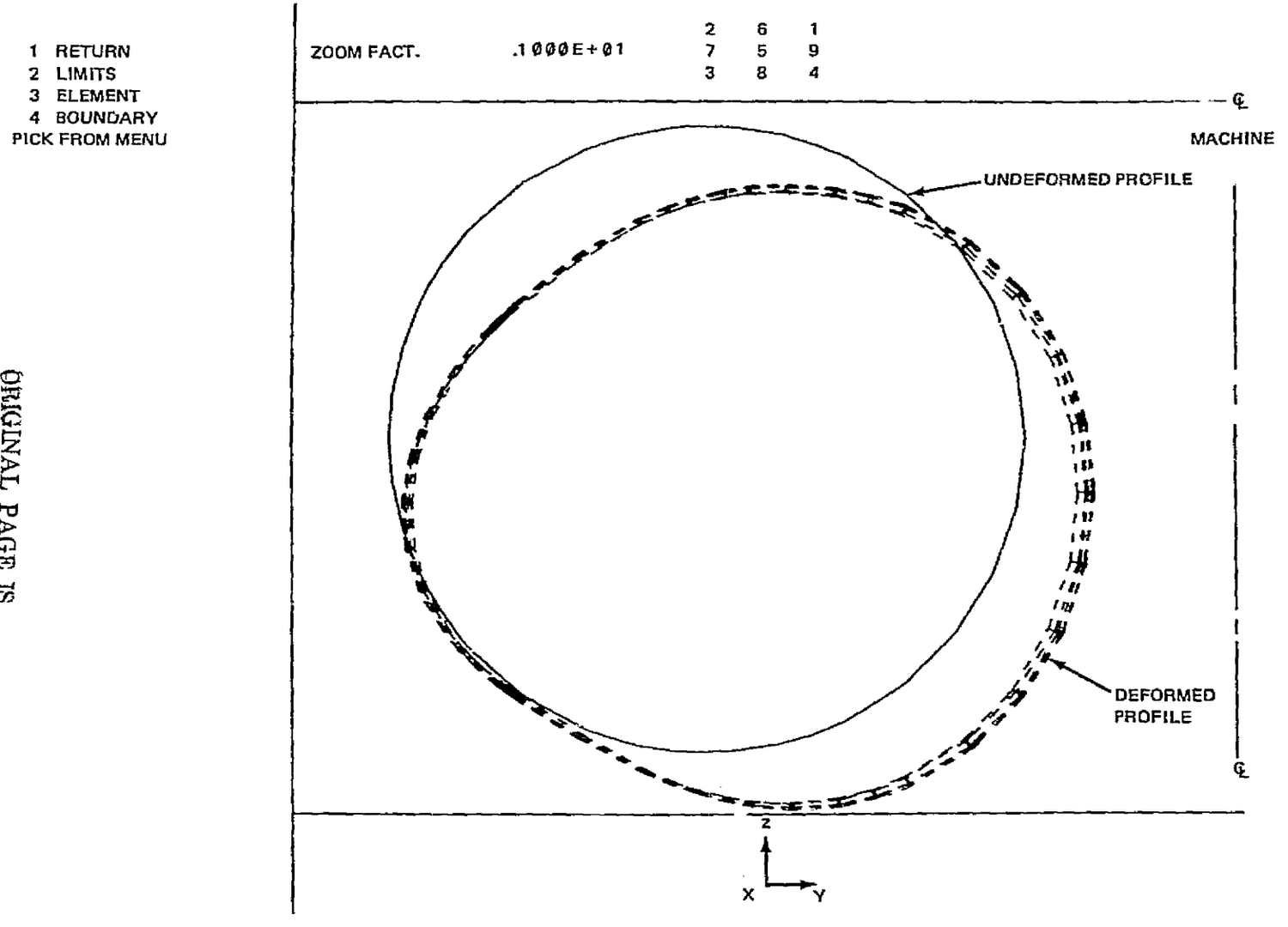

2036-012

Figure 12 Deformed and Undeformed Profiles of Bellows Case 1

2036-013

Figure 13 Deformed and Undeformed Profiles of Bellows Case 2

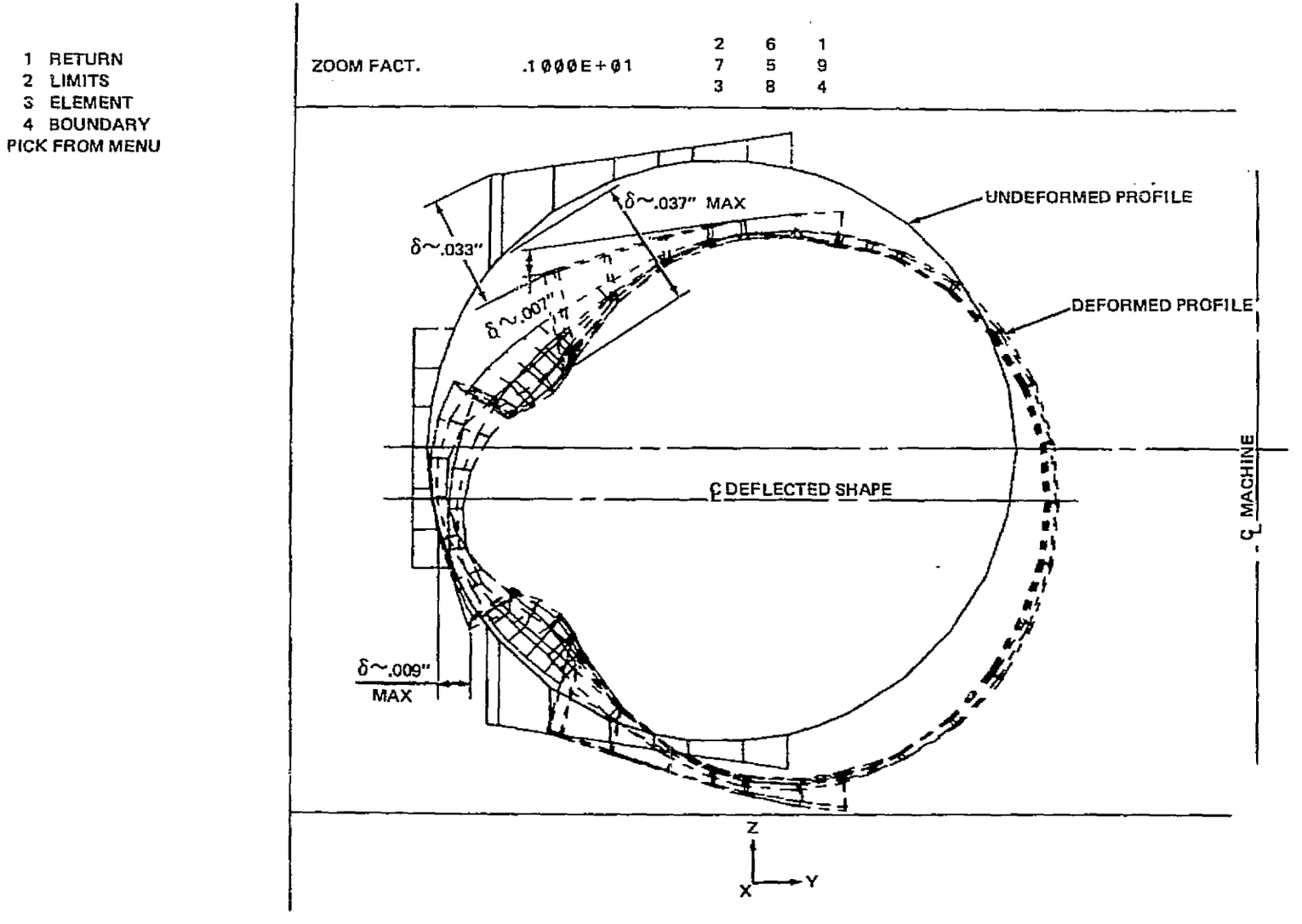

Figure 14 Deformed and Undeformed Profiles of Pie 2

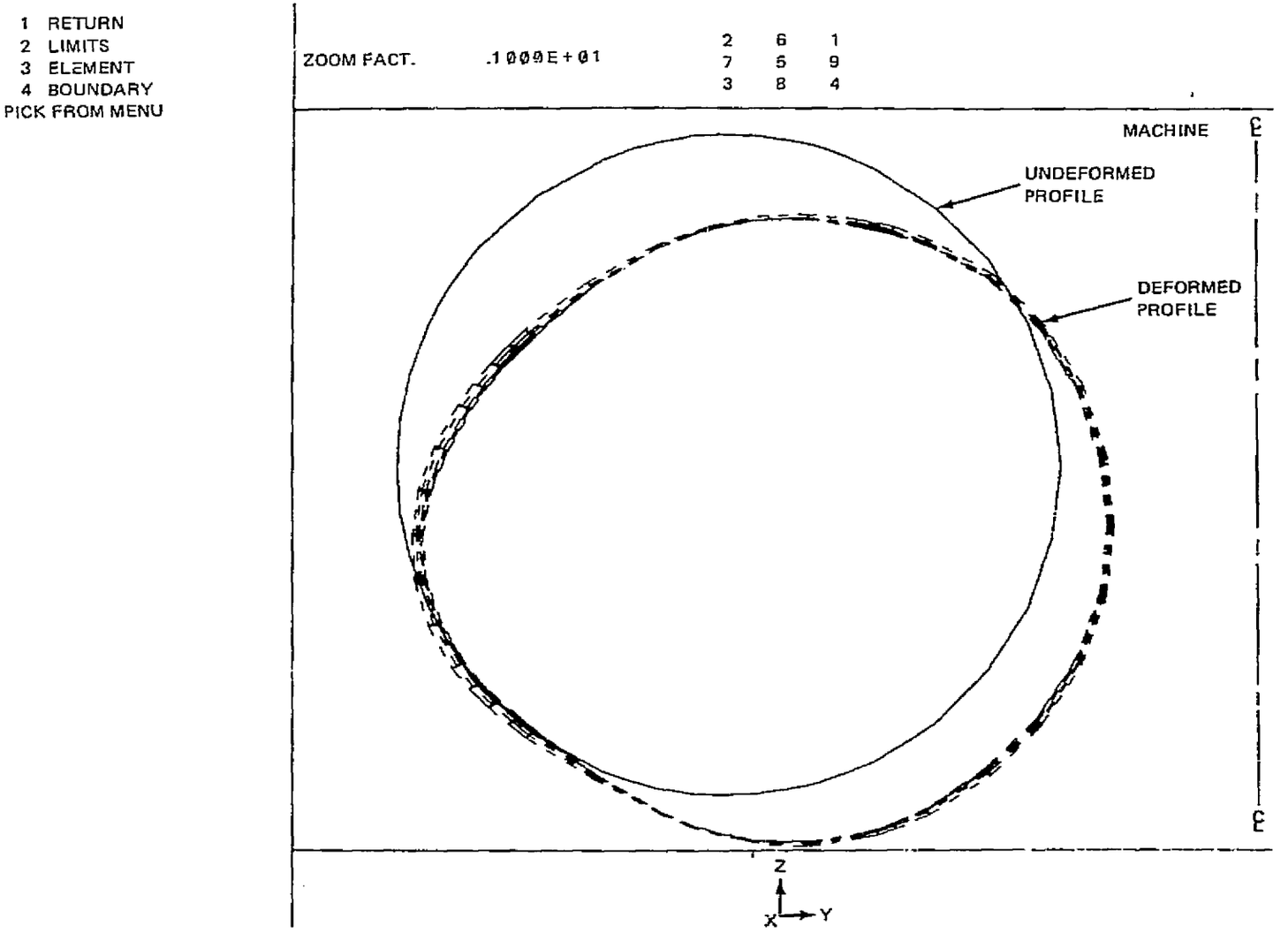

2036-015

Figure 15 Deformed and Undeformed Profiles of Pie 1 and the Parting Plane

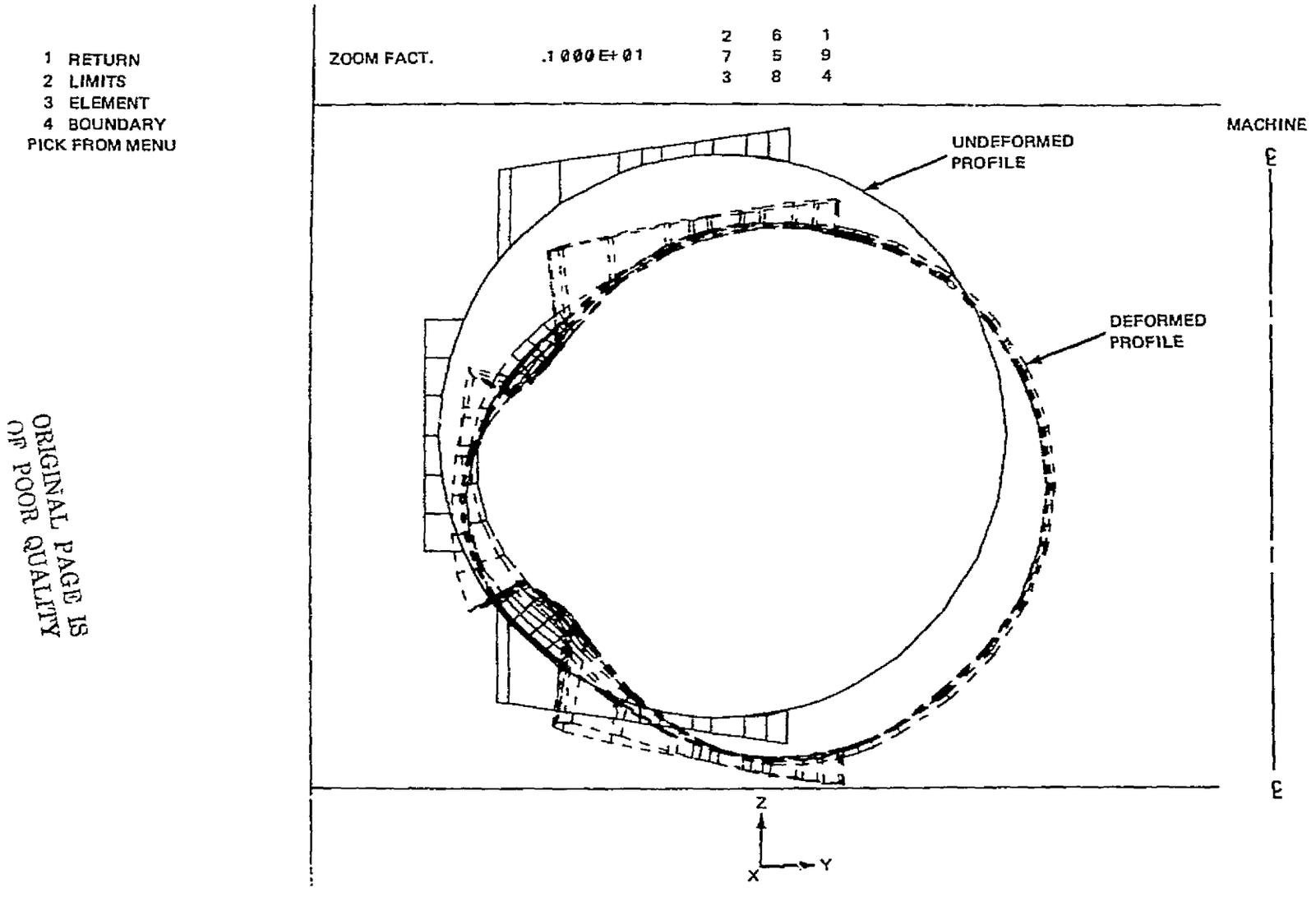

Figure 16 Deformed and Undeformed Profiles of Pie 3